

# Quick Detection of Formation of Protective Scales on Heat-resistant Steels in High-temperature Oxidation

Toshio MARUYAMA

Professor, Department of Metallurgy and Ceramics Science

Tokyo Institute of Technology

## 1. Introduction

Operation at the higher temperature in plants for power generation offers the higher efficiency and the reduction of CO<sub>2</sub> emission. The target temperature is 700 °C. To achieve this, materials with high creep strength are required so that researches are conducted on ferritic Fe-Cr steels, austenitic alloys and nickel-based superalloys. On the other hand, the high-temperature operation may give problems of the material degradation by high-temperature oxidation/corrosion which determines the life of plants. When the oxide scales is iron oxides, the oxidation rate is too high at 700 °C. The formation of the external Cr<sub>2</sub>O<sub>3</sub> scale is required. The present authors have reported the effect of water vapor on the internal/external oxidation in Fe-Cr alloys by microstructure observation<sup>1,2)</sup>.

The decrease of oxidation rate and suppression of spalling are important issues, which depend on the protectiveness of scales. In chromium-bearing heat-resisting steels, the Cr contents affect the microstructure of scales. The development of a technique is expected to evaluate quickly the protectiveness of the scale and feedback the results to the alloy design and the proper operation.

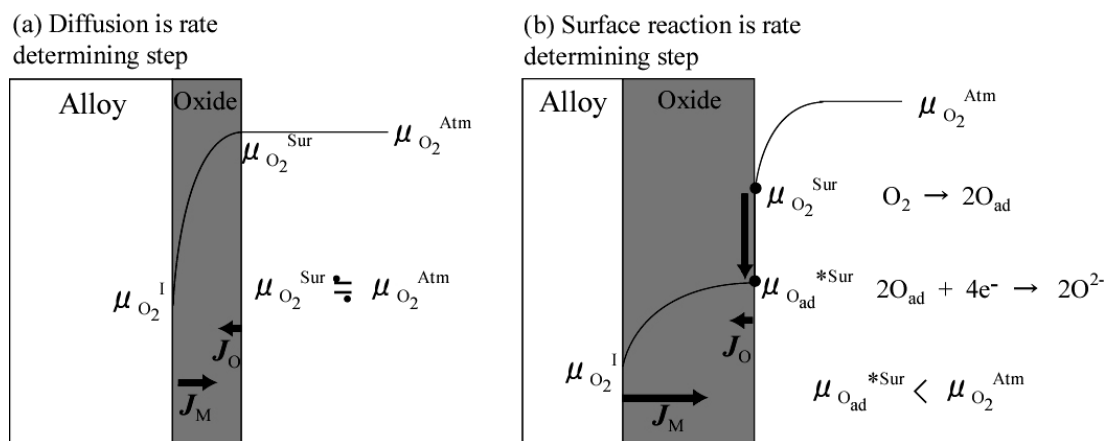


Fig. 1 Schematic diagram of potential distribution of oxygen in oxide scale.

As shown in Fig.1 (a), the formation of protective  $\text{Cr}_2\text{O}_3$  scale provides the oxygen potential at the surface of the scale to be closed to that in the atmosphere because diffusion through the scale is the rate-determining step. On the other hand, the formation of less protective scales with high ionic diffusivity such as  $\text{FeO}$  gives lower oxygen potential at the surface than that in the atmosphere because the supply of oxidant in the gaseous boundary layer is rate determining (Fig.1 (b)). The measurement of oxygen potential at the surface offers the technique to evaluate the protectiveness of the scales.

The principle and the experimental set-up have been reported elsewhere<sup>3)</sup>. In the paper, the technique was applied to high temperature oxidation of nickel, cobalt and iron at 1373 K and was confirmed the validity. In the present paper, the usefulness of this technique was demonstrated in the detection of formation of protective scales on heat-resistant steels in high-temperature oxidation.

## 2. Principle<sup>3)</sup>

Calcia-stabilized  $\text{ZrO}_2$  (CSZ) is known as an oxide ion conductor, and is often used as an electrolyte of an potentiometric oxygen sensor. When CSZ is exposed to a difference of oxygen chemical potential, an electromotive force is generated. In this study, the oxygen concentration cell shown in Fig. 2 is proposed in order to measure the difference of the oxygen chemical potential between at the oxide surface and in the atmosphere during the high temperature oxidation of a metal. A metal sheet welded a platinum lead is placed on a CSZ bar attached with a platinum lead on the other side as shown in Fig. 2(a).

When the cell is exposed to the oxidizing atmosphere at elevated temperatures, the oxide scale is formed on the metal. In the case that the scale is in the scale. On the other hand, when growth proceeds outward as shown in Fig. 2(b), the CSZ bar is partly embedded the scale growth proceeds inward (Fig. 2(c)), the CSZ bar is always attached on the scale surface.

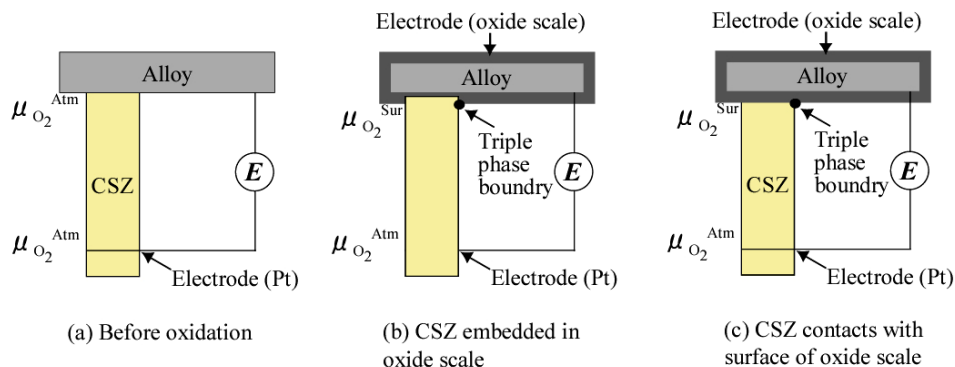
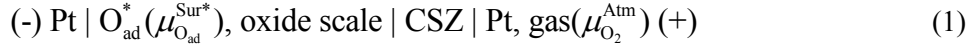


Fig. 2 Oxygen concentration cell for the measurement of surface oxygen potential.

When the oxide scale is an electronic conductor, the oxide scale itself behaves as an electrode of the cell. The redox reaction of oxygen mostly occurs at the triple phase boundary of CSZ, electrode of the scale and gas phase. The cell is expressed as



where  $\mu_{\text{O}_{\text{ad}}}^{\text{Sur}*}$  and  $\mu_{\text{O}_2}^{\text{Atm}}$  denote the oxygen chemical potentials of the adsorbed oxygen atom at the oxide surface and oxygen molecule in the atmosphere, respectively. The electrochemical reaction at the electrode in the atmosphere is



and that at the oxide surface is



The electromotive force of this cell,  $E_{\text{cell}}$  is expressed as,

$$E_{\text{cell}} = -(2\mu_{\text{O}_{\text{ad}}}^{\text{Sur}*} - \mu_{\text{O}_2}^{\text{Atm}}) / 4F = (RT / 4F) \ln(P_{\text{O}_2}^{\text{Atm}} / P_{\text{O}_2}^{\text{Sur}}) \quad (4)$$

where  $F$  is the Faraday constant.  $P_{\text{O}_2}^{\text{Atm}}$  and  $P_{\text{O}_2}^{\text{Sur}}$  denote the oxygen partial pressure in the atmosphere and that at the oxide surface, which relates to the oxygen chemical potentials of the adsorbed oxygen atom in the following manner.

$$2\mu_{\text{O}_{\text{ad}}}^{\text{Sur}*} = \mu_{\text{O}_2}^{\circ} + RT \ln(P_{\text{O}_2}^{\text{Sur}*}) \quad (5)$$

The eq. (4) gives the oxygen chemical potential at the oxide surface from  $E_{\text{cell}}$  and  $\mu_{\text{O}_2}^{\text{Atm}}$ .

In the case of Fig. 2 (b), the redox reaction of oxygen occurs at embedded part of CSZ and at the triple phase boundary at the surface. Therefore, the electric potential of the oxide scale (electrode) is a mixed potential. The mixed potential of the oxide scale can be obtained as that which the anodic current and the cathodic current are identical. The anodic reaction occurs much more at the triple phase boundary of CSZ, where the oxygen transport is extremely higher than the scale interior. Therefore, the mixed potential is just slightly lower than the oxygen potential at the triple phase boundary. However, the difference is considered to be negligibly small.

### 3. Experimental

#### 3.1 Experimental set-up

Figure 3 shows a schematic illustration of experimental set-up and the oxygen concentration cell. In order not only to support the metal coupon but also to ensure the free gas flow, the CSZ tube was cut into the shape as shown in Fig. 3(b), which has three bars. The platinum electrode detecting the oxygen potential in the atmosphere is attached at the position of 20 mm away from the sample to make the position to be outside of the boundary layer. A CSZ oxygen sensor is located beneath the cell in order to monitor the oxygen chemical potential in the atmosphere,  $\mu_{O_2}^{Atm}$ . The reference electrode of this sensor is air.

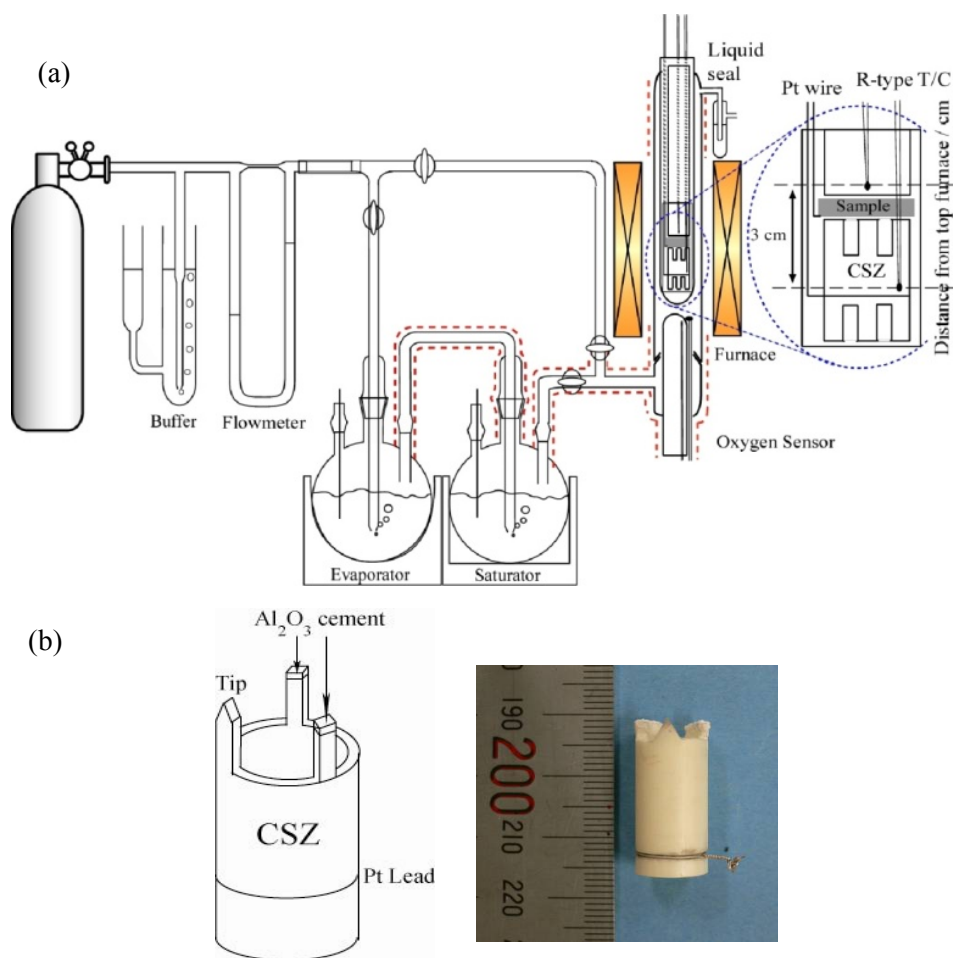


Fig. 3 Experimental set-up for the measurement of surface oxygen potential.

(a) whole system and (b) cell.

The electromotive force of the oxygen sensor,  $E_{\text{sensor}}$  is expressed as,

$$E_{\text{sensor}} = -(\mu_{\text{O}_2}^{\text{Atm}} - \mu_{\text{O}_2}^{\text{Air}}) / 4F = (RT / 4F) \ln(P_{\text{O}_2}^{\text{Air}} / P_{\text{O}_2}^{\text{Atm}}) \quad (6)$$

where  $\mu_{\text{O}_2}^{\text{Air}}$  and  $P_{\text{O}_2}^{\text{Air}}$  denote the oxygen chemical potential and the oxygen partial pressure in air. Both the cell and the CSZ oxygen sensor should be located in the isothermal zone of the furnace to minimize errors caused by thermo-electromotive force of CSZ and temperature dependence of gas phase equilibrium. The temperatures at the metal coupon and at the oxygen sensor were monitored during oxidation experiments by thermocouples (T. C. ) of type -R that were placed as shown in Fig. 3(a).

## 3.2 Experimental procedure

### 3.2.1 Sample

The plates (10x10x1 mm<sup>3</sup> in size) of samples of Fe-5~25 mass% Cr were used after annealing at 1473 K for 43.2 ks (12h) in vacuum.

### 3.2.2 High Temperature Oxidation

Dry oxidation was carried out in the stream of Ar-21% O<sub>2</sub> gas mixture up to 20 ks. The oxygen partial pressure of the Ar-21%O<sub>2</sub> gas mixture was checked by a CSZ oxygen sensor before the test furnace and was about 2.1x10<sup>4</sup> Pa at 973 K.

Steam oxidation was carried out at 973 K in the stream of Ar-30%H<sub>2</sub>O gas mixture (the dew point of 351 K) up to 20 ks. The atmosphere of Ar-30%H<sub>2</sub>O gas mixture was obtained by bubbling purified Ar gas through the evaporator and the saturator both containing distilled water. The evaporator was held at 355 K by a heating mantle and the saturator was maintained at 351 ± 1 K by a water bath. The gas flow was controlled to the flow rate of 100 cm<sup>3</sup> min<sup>-1</sup>. The oxygen partial pressure of the Ar-30%H<sub>2</sub>O gas mixture was checked by a CSZ oxygen sensor before the test furnace and was about 6x10<sup>-9</sup> Pa at 973 K.

### 3.2.3 Analysis

After the oxidation, the furnace was cooled down to room temperature. For observation of cross section, the samples were mounted in epoxy resin, ground by SiC abrasive paper up to #2000 grits, and polished by 4 μm diamond slurry. The cross sections were observed by scanning electron microscope (SEM) and EPMA. Phases in the oxide were identified by X-ray diffraction (XRD).

## 4. Results

### 4.1 Oxidation in dry condition (Ar-21%O<sub>2</sub>)

Figure 4 shows the oxygen chemical potentials at the surface of growing scale with that in the atmosphere calculated from the emfs of the cell and sensor during oxidation in Ar-21%O<sub>2</sub> mixed gas. The oxygen chemical potential at coexistence of oxides of Fe<sub>3</sub>O<sub>4</sub>/Fe<sub>2</sub>O<sub>3</sub> equilibrium calculated from thermodynamic data of Barin<sup>4)</sup> are also shown in the figure. The oxygen chemical potential on the surface of Fe-5Cr is lower by 3~4 orders of magnitudes than that in the atmosphere and the difference decreases gradually with oxidation time. In the case of Fe-9Cr, the surface oxygen potential is lower by 2 orders of magnitudes than that in the atmosphere. On the other hand, the surface oxygen potentials of Fe-12Cr and 15Cr are close to oxygen potential in the atmosphere.

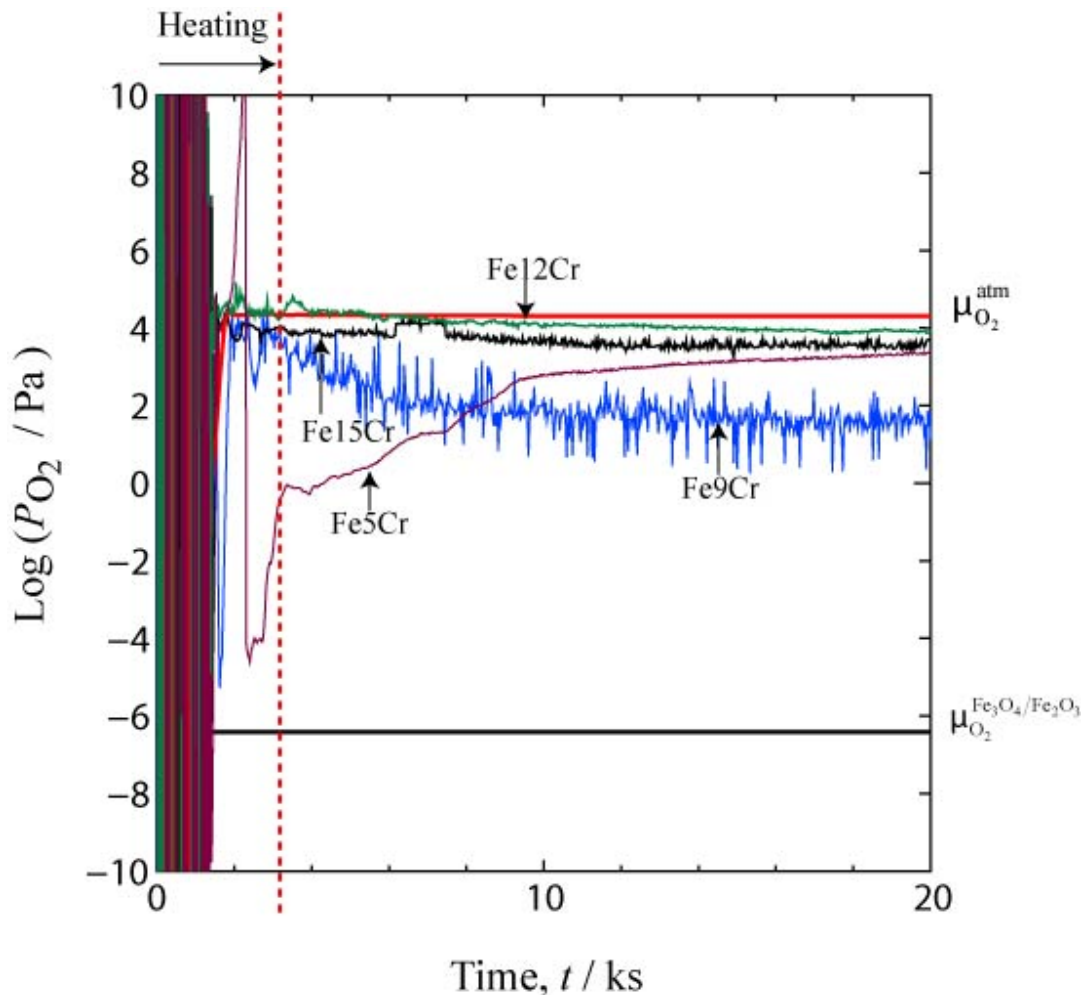


Fig. 4 Oxygen chemical potentials at the surface of growing scale

#### 4.2 Oxidation in humid condition (Ar-30%H<sub>2</sub>O)

Figure 5 shows the oxygen chemical potentials at the surface of growing scale in Ar-30%H<sub>2</sub>O mixed gas. The oxygen chemical potentials at coexistence of oxides of Cr/Cr<sub>2</sub>O<sub>3</sub>, Fe/FeCr<sub>2</sub>O<sub>4</sub>/Cr<sub>2</sub>O<sub>3</sub>, Fe/FeO, FeO/Fe<sub>3</sub>O<sub>4</sub> and Fe<sub>3</sub>O<sub>4</sub>/Fe<sub>2</sub>O<sub>3</sub> calculated from thermodynamic data of Barin<sup>4)</sup> are also shown. The oxygen chemical potential on the surface of oxide scales in Fe-5~15 Cr drops down more than 5 orders of magnitudes from the oxygen potential at the atmosphere, which are below the oxygen chemical potential of FeO/Fe<sub>3</sub>O<sub>4</sub> equilibrium. On the other hand, the oxygen chemical potentials on the surfaces of oxide scales in Fe-20 and 25 Cr alloy are close to the oxygen potential at the atmosphere.

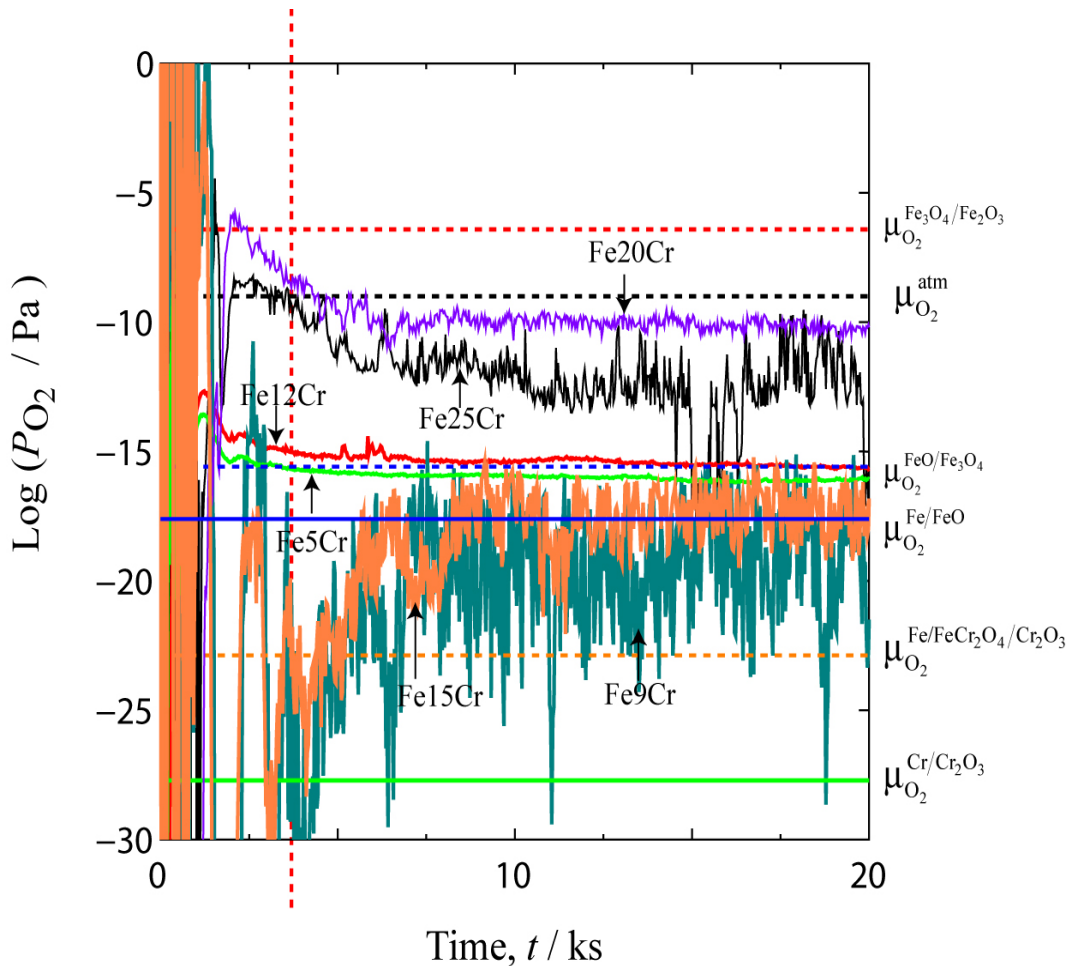


Fig. 5 Oxygen chemical potentials at the surface of growing scale

### 4.3 Microstructure and phases in oxide scales

Figure 6 shows cross sections of Fe-15 and -25 Cr alloys after oxidation at 973 K for 20 ks in Ar-30% H<sub>2</sub>O. It is clearly observed that a thick duplex scale forms on Fe-15 Cr alloy and a thin external scale exists on Fe-25 Cr alloy.

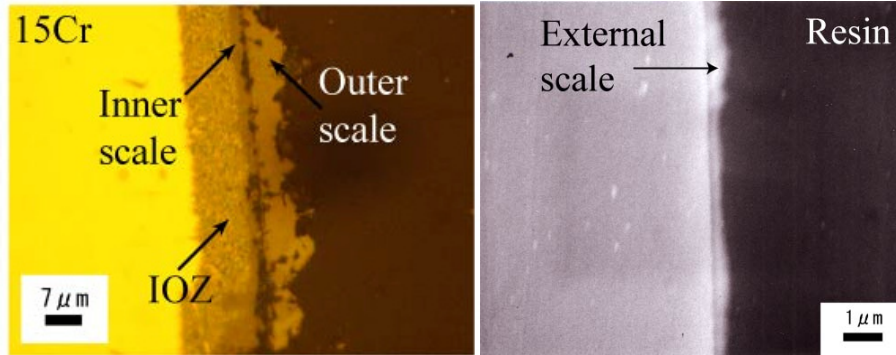


Fig. 6 Cross sections of oxide scales formed on Ar-30%H<sub>2</sub>O mixture.

Figure 7 illustrates the XRD patterns of the sample surfaces after oxidation for 20 ks. In dry oxidation (Ar-21%O<sub>2</sub>), the peaks of  $\alpha$ -Fe and Cr<sub>2</sub>O<sub>3</sub> appear in Fe-9~15Cr alloys. Fe<sub>2</sub>O<sub>3</sub> peak was detected only in the sample of Fe-5mass%Cr. On the other hand, oxidation in Ar-30% H<sub>2</sub>O gives peaks of  $\alpha$ -Fe, FeO and FeCr<sub>2</sub>O<sub>4</sub> spinel in Fe-5Cr but only Cr<sub>2</sub>O<sub>3</sub> appears as the oxide phase in Fe-25 Cr. The stronger intensity of the peak of  $\alpha$ -Fe for the metal substrate indicates the thinner oxide scales.

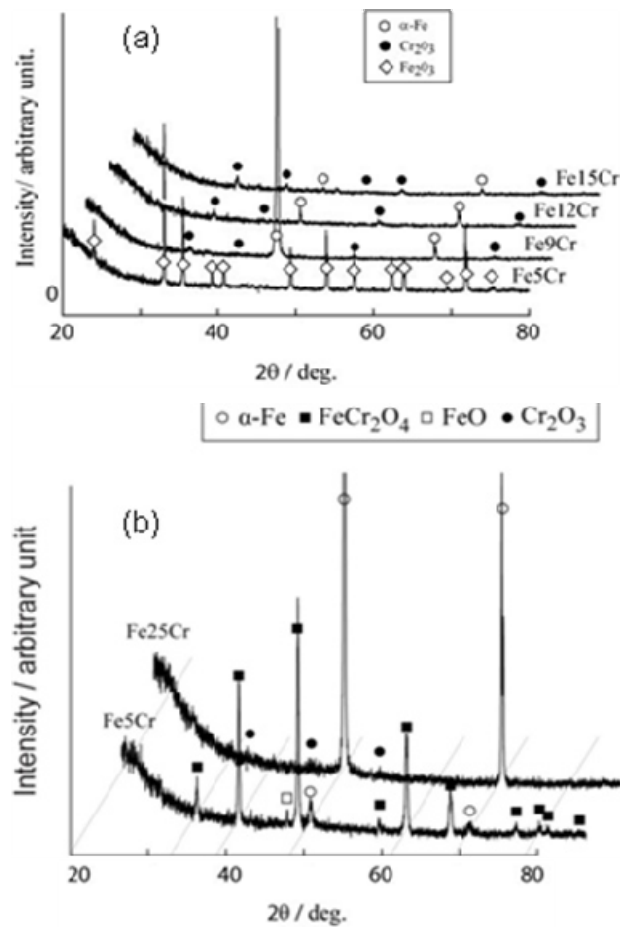


Fig. 7 XRD patterns of the sample surfaces after oxidation for 20 ks

## 5. Discussion

### 5.1 Surface oxygen potential measurement

The surface oxygen potential at growing scales is lowered by consumption of oxygen by oxidation. The samples contain Cr of which concentration is high enough to form a protective external  $\text{Cr}_2\text{O}_3$  scale exhibit the surface oxygen potential to be close to that in the atmosphere. This technique is very useful in quick detection of formation of protective scales.

The prominent difference in surface oxygen potential between dry and humid atmospheres is the fluctuation in potentials. The fluctuation in humid atmosphere (Fig. 5) is larger than that in dry atmosphere (Fig. 4). Schutze et al.<sup>5)</sup> carried out the acoustic emission (AE) measurement during high temperature oxidation of Fe-Cr steels and reported that AE event / signal was dramatically increased in humid oxidation compared to in dry oxidation. They proposed that the presence of water vapor increases the growth stress in the scales and leads to the formation of crack. The fluctuation of surface potentials may be caused by the scale cracking during oxidation.

### 5.2 Effect of water vapor on Cr concentration required to form an external $\text{Cr}_2\text{O}_3$ scale.

Figure 8 summarizes the mode of oxidation for Fe-Cr alloys in dry and humid atmosphere at 973 K. The blank and solid squares denote the formation of external  $\text{Cr}_2\text{O}_3$  scale and the formation of iron-based oxide scale without protective  $\text{Cr}_2\text{O}_3$  scale, respectively. The left two results were obtained at oxygen pressure of  $4.3 \times 10^{-17}$  Pa<sup>5)</sup>. The required Cr concentration is 8~9 mass% in dry condition. The water vapor in atmospheres increases the Cr concentration to 12 mass%

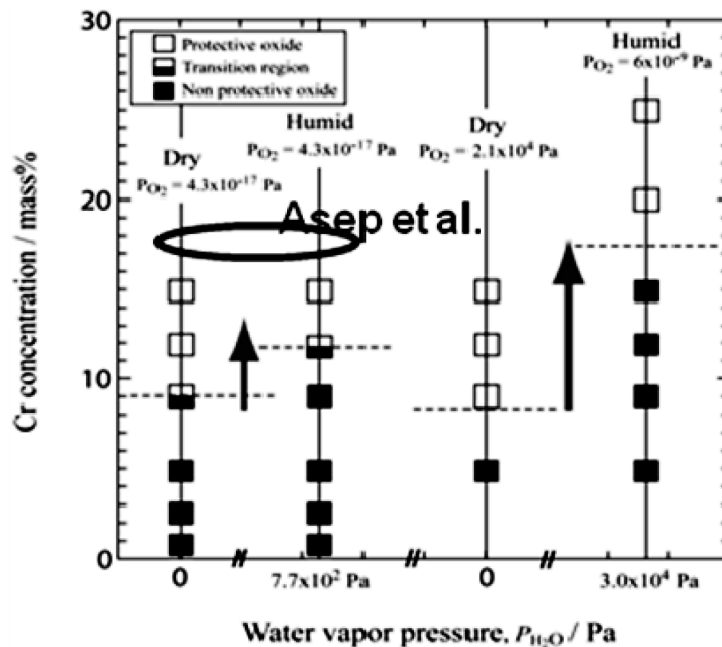


Fig. 8 Mode of oxidation for Fe-Cr alloys in dry and humid atmosphere at 973 K. (the left half was from Asep et al.<sup>6)</sup>)

at oxygen pressure of  $4.3 \times 10^{-17}$  Pa and water vapor pressure of  $7.7 \times 10^2$  Pa. The increase of water vapor pressure to  $3 \times 10^4$  Pa requires Cr concentration of 18 mass%. The water vapor in atmosphere affects strongly the formation of external  $\text{Cr}_2\text{O}_3$  scale.

## 6. Conclusion

The continuous measurement of chemical potential of oxygen at the surface of growing scale was applied to the investigation to clarify the effect of water vapor in high temperature oxidation of Fe-Cr alloys. This technique successively provided the surface oxygen potential which is a measure of the protectiveness of scales and the indication of the formation of external  $\text{Cr}_2\text{O}_3$  scale. The water vapor in atmosphere affects strongly the formation of external  $\text{Cr}_2\text{O}_3$  scale in high temperature oxidation of Fe-Cr alloys..

## Acknowledgement

This study was supported in part by JFE 21<sup>st</sup> Century Foundation in 2008.

## References

- 1) M. Hanafi, T. Kodama, M. Ueda, K. Kawamura, T. Maruyama, *Mater. Trans.*, **50** (11), 2656 (2009).
- 2) A.R. Setiawan, M. Hanafi, M. Ueda, K. Kawamura, T. Maruyama, *ISIJ Int.*, **50** (2), 259(2010).
- 3) Kojiro Akiba, Mitsutoshi Ueda, Kenichi Kawamura and Toshio Maruyama, *Materials Transactions*, **49**(3), 629 (2008).
- 4) Barin, *Thermochemical Data of Pure Substances*, VHC Publisher, Vol. **4**, (1991).
- 5) M. Schutze, D. Rensch and M. Schorr, *Corrosion Engineering, Science and Technology*, **39**(2), 157 (2004).
- 6) A.R. Setiawan, M. Ueda, K. Kawamura, T. Maruyama, *Oxidation of Metals*, (to be submitted).